



## Study on Thermal Performance of the Small-Scale Air Conditioning with Thermoelectric Cooling Module

Sahassawas Poojeera<sup>1</sup>, Aphichat Srichat<sup>2</sup>, Nittaya Naphon<sup>3</sup>, Paisarn Naphon<sup>4\*</sup>

<sup>1</sup> Department of Mechanical Engineering, Faculty of Engineering, Rajamangala University of Technology, Khon Kaen Campus, Khon Kaen 40000, Thailand

<sup>2</sup> Department of Mechanical Engineering, Faculty of Technology, Udon Thani Rajabhat University, Udon Thani 41000, Thailand

<sup>3</sup> Department of Pharmaceutical Chemistry, Faculty of Pharmacy, Srinakharinwirot University, Nakhorn-Nayok 26120, Thailand

<sup>4</sup> Thermo-Fluids and Heat Transfer Enhancement Research Lab (TFHT), Department of Mechanical Engineering, Faculty of Engineering, Srinakharinwirot University, Nakhorn-Nayok 26120, Thailand

Corresponding Author Email: [paisarnn@g.swu.ac.th](mailto:paisarnn@g.swu.ac.th)

Special Issue: Hybrid Renewable Energy Systems and Integration

<https://doi.org/10.18280/mmep.090434>

### ABSTRACT

**Received:** 25 June 2022

**Accepted:** 9 August 2022

#### Keywords:

*thermoelectric cooling module, thermal performance improvement, air conditioning system*

This work presents the COP and EER of the combined air conditioning and thermoelectric cooling systems. The small-scale air conditioning (8000 BTU/hr) with thermoelectric cooling systems is set up in the closed room (2.0\*2.0\*2.0 m), and free energy from the photovoltaic cell is used for the thermoelectric cooling module. The COP and EER with the thermoelectric cooling module are higher than those without the thermoelectric cooling module. It is observed that the COP and EER increase as the axial fan speeds increase. In addition, there is good agreement from the comparison, giving an average error of 3.77%. The highest COP and EER for the system with the thermoelectric cooling module are 1.71 and 5.85 for an airflow rate of 4.7 m<sup>3</sup>/s, respectively. The results can be used as guidelines for developing the thermal performance of air conditioning by combining it with the thermoelectric cooling module.

## 1. INTRODUCTION

Due to global warming, the use of air conditioning systems is rapidly increasing, affecting higher energy requirements. Meanwhile, air conditioning systems have been developed continuously to obtain higher efficiency and lower power consumption. Today, many cooling systems use thermoelectric as a cooler to enhance cooling ability in the systems. However, the cooling ability of thermoelectrics depends on many relevant parameters that must be studied continuously, which many papers presented on thermoelectric applications due to many advantages [1]. Domestic refrigerators [2] have low thermal efficiency than vapor compression refrigeration systems [3, 4]. Thermoelectric refrigerators can be installed in confined spaces. Portable coolers are likely to be used outdoors, either battery-powered or powered by solar panels. The thermal performance of the portable refrigerators is < 0.5 for an operating temperature difference of 20-25°C. Min and Rowe [4] determined the thermoelectric domestic refrigerators, for which the obtained COP was 0.3-0.5 at a 20°C inside/outside temperature difference. Next, the portable thermoelectric refrigerator driven by photovoltaic cells has been investigated [5-7]. The results found that the coefficient of performance was about 0.23. Astrain et al. [8] studied the combined thermoelectric and vapor compression hybrid refrigerator. The efficiency of

a system with ionic wind fans has been developed [9]. Electronic devices generate much heat during operation, so the maximum junction temperature should be maintained below 85°C [10], and the maximum generated heat is about 200W [11]. Naphon and Wiriyasart [12] developed the thermoelectric cooling module for the CPU using nanofluids as coolants. Nanofluids have a significant choice better than water for the coolant in the cooling system [13, 14].

Thermoelectric coolers have many advantages, such as having a small size, no moving parts, coolant flowing in the system flexible power supply of the electric vehicle system. Therefore, a cooler has been applied for automotive applications [15]. Qinghai et al. [16] studied the efficiency of a cooler. Optimizing the COP of the cooler [17, 18] and the coolers/power generators for automobiles [19] have been performed. Next, Srivastava et al. [20] numerically analyzed vehicle cabins with solar-assisted thermoelectric cooling/heating systems. Riffat and Qiu [21] studied the efficiency of thermoelectric and conventional coolers. The average COPs are 2.8 and 0.42, respectively, for conventional air conditioning and thermoelectric coolers.

Cosnier et al. [22] studied the cooler systems by using thermoelectric. Next, Cheng et al. [23] designed a cooler system driven by photovoltaic cells at a temperature difference of 16.2°C. Gillott et al. [24] studied thermoelectric cooling system buildings. Active thermal windows and active

thermoelectric walls for the room have been introduced by Arenas et al. [25] and Vázquez et al. [26]. Shen et al. [27] studied thermoelectric air conditioning. The maximum COP of 1.77. Cherkez [28] applied the on cooling thermoelements for the thermoelectric cooler unit with the COP increases 1.6-1.7 times. Miranda et al. [29] applied the green energy-powered thermoelectric for the air conditioning. Shen et al. [30] studied a cooling system and thermoelectric air conditioning-driven photovoltaic cells with a hot water supply [31]. Next, Attar and Lee [32] designed the cooler system with TCM, and the results validated the analytical analysis. Li et al. [33] considered the energy management system of TCM. Irshad et al. [34] presented a sizing and cost of an air duct with solar cell calculations. Next, the thermoelectric air conditioning undergarment for HVAC energy saving has been considered [35]. Tian et al. [36] proposed the tube arrangement of the thermoelectric module as an air cooler. Duan et al. [37] studied thermoelectric systems and a solar-driven thermoelectric unit with and without dehumidifiers [38, 39]. Next, Salehi et al. [40] determined the efficiency of the solar cooling modules. Han et al. [41] studied the efficiency of a TCM using liquid as a coolant and a TCM [42]. Saini et al. [43] presented an air conditioning system with a thermoelectric module. Next, Almodfer et al. [44] used the random vector to determine the efficiency of a solar-powered thermoelectric cooler. The most productive studies have been continuously done [45-53]. They apply the thermoelectric cooling module for many systems, including; cold-hot water dispensers [45, 46], sensible air cool-warm fan [47], liquid cooler module [48], cooling CPU [49], electric generator [50], the cooling module with nanofluid as coolant [51], and cooling electrical vehicle battery module [52, 53]. The thermoelectric cooling modules use water and nanofluids as working fluids flowing through the systems.

As reviewed above, many papers presented the thermoelectric application areas. The thermoelectric has many advantages, including; a small scale, various coolants, and a quiet operating sound. However, some disadvantages are the expensive and low performance. This paper aims to analyze the thermal performance of the small-scale combined air conditioning and thermoelectric cooling system. Obtained from this study, the combined air conditioning and thermoelectric cooling module have affected the increasing COP and EER of the combined small-scale air conditioning system.

## 2. EXPERIMENTAL APPARATUS AND METHOD

### 2.1 Test loop

As shown in Figure 1 (A), the present test loop consists of the air conditioning system, four thermoelectric modules, a closed room, and an operating control system. The structure of the closed space (2.0 m\*2.0 m\*2.0 m) is assembled from an aluminum profile, and the walls are made from plywood and covered with an insulator sheet to decrease heat loss. Four thermoelectric cooling modules are installed at the wall as the supplied air duct of the air conditioning system. There are many ways of thermoelectric refrigeration, such as lithium bromide technology and semiconductor refrigeration technology for a cooling system. However, the reason for choosing a thermoelectric air-cooling module for air cooling is because the experiment's system combined the air

conditioning system with a thermoelectric air-cooling module. The thermoelectric plate has some advantages, including a small scale, easily switching between heating and cooling modes, and a quiet operating environment. The photovoltaic-thermoelectric cooling system consists of four modules, a DC battery (12V, 80Ah), a photovoltaic cell, a charger controller, and an inverter. The hourly variation of the solar radiation on the horizontal surface outside reaches 1000 W/m<sup>2</sup> [54]. Each thermoelectric cooling module consists of four axial fans, three heat sink units, and two thermoelectric plates (12.3V). The total ampere of the thermoelectric cooling module is about 25.6A. Therefore, electrical DC power requires about 12.3x25.6 = 314.88W, and a photovoltaic cell is 450W. Each side of the thermoelectric plate is attached by high thermal conductivity special glue to the heat sink unit, as shown in Figure 2. The thermoelectric plate has an operating temperature of 70°C and a cooling capacity of 60W. Type T thermocouples measure the cold-hot surface temperatures, and twelve thermocouples are used to measure the air temperature in three levels (4 points), as shown in Figure 1(B), controlled by the Arduino control system.

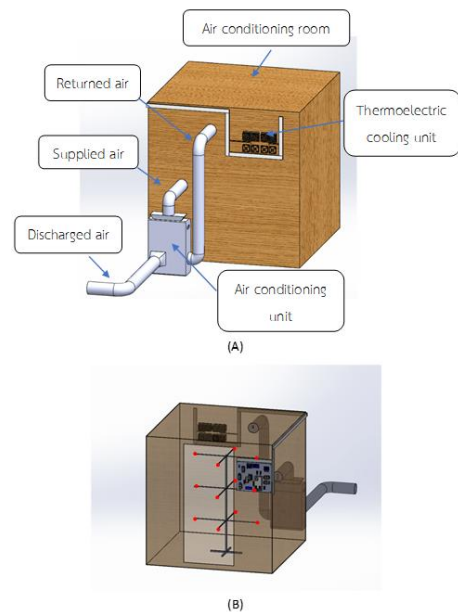


**Figure 1.** Schematic diagram of (A) the air conditioning room and (B) air temperature measurement positions

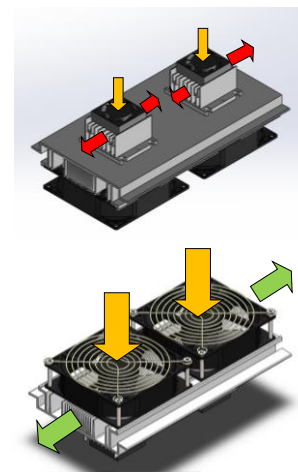


**Figure 2.** Schematic diagram of thermoelectric cooling module used in the present study

## 2.2 Data reduction and uncertainty analysis

The cooling capacity of the air conditioning system and the thermoelectric cooling module are calculated from

$$Q_{c.AC} = \dot{m}_{a1} (h_{st1} - h_{fi1}) \quad (1)$$

$$Q_{c.TCM} = \dot{m}_{a2} (h_{st2} - h_{fi2}) \quad (2)$$

The energy requirement of the thermoelectric cooling module includes the power of axial fans and thermoelectric plate as follows:

$$P_{TCM} = P_{fh} + P_{fc} + P_{TP} \quad (3)$$

The energy efficiency of the TCM is presented in terms of the COP as follows:

$$COP_{TCM} = \frac{Q_{c.TCM}}{P_{TCM}} \quad (4)$$

The COP of the air conditioning system and energy efficiency ratio is calculated from

$$COP_{AC} = \frac{Q_{c.AC}}{P_{AC}} \quad (5)$$

$$EER_{without} = 3.14COP_{without} \quad (6)$$

In the present study, energy from the photovoltaic cell for the thermoelectric cooling system is free energy. Therefore, it is not included in the overall coefficient of performance (COP) calculation process, which is calculated from

$$COP_{OV} = \frac{Q_{c.TCM} + Q_{c.AC}}{P_{TCM} + P_{AC}} \quad (7)$$

$$= \frac{\dot{m}_{a2} (h_{st2} - h_{fi2}) + \dot{m}_{a1} (h_{st1} - h_{fi1})}{(P_{fh} + P_{fc} + P_{TP}) + P_{AC}}$$

**Table 1.** Accuracy and uncertainty of measurements

Instrument	Accuracy (%)	Uncertainty
Anemometer	0.1	±0.2
Dry-box temperature calibrator	0.1	±0.1
DHT22 temperature	0.1	±0.1
DC voltage and current sensor	0.1	±0.01
AC digital power energy meter	0.1	±0.01

Based on the errors of the instruments (Table 1), the uncertainty estimation process has been performed [55]. The maximum uncertainty value of the COP is ± 7.5%, which is calculated as follows:

$$Uncertainty\ y = \sqrt{\left(\frac{\partial COP}{\partial h_{st1}} \Delta h_{st1}\right)^2 + \left(\frac{\partial COP}{\partial h_{fi1}} \Delta h_{fi1}\right)^2 + \left(\frac{\partial COP}{\partial h_{st2}} \Delta h_{st2}\right)^2 + \left(\frac{\partial COP}{\partial h_{fi2}} \Delta h_{fi2}\right)^2 + \left(\frac{\partial COP}{\partial \dot{m}_{a1}} \Delta \dot{m}_{a1}\right)^2 + \left(\frac{\partial COP}{\partial \dot{m}_{a2}} \Delta \dot{m}_{a2}\right)^2 + \left(\frac{\partial COP}{\partial P_{AC}} \Delta P_{AC}\right)^2 + \left(\frac{\partial COP}{\partial P_{TCM}} \Delta P_{TCM}\right)^2} \quad (8)$$

## 3. MATHEMATICAL MODELING

In a computational process, an air conditioning system with and without thermoelectric cooling modules is investigated numerically with dimensions and the mains computation domains, as shown in Figure 3. The turbulent flow model is used to consider the problems. The main governing equations are given as follows [56, 57]:

$$\frac{\partial \rho}{\partial t} + \text{div}(\rho \mathbf{U}) = 0 \quad (9)$$

$$\rho \frac{D\mathbf{U}}{Dt} = -\frac{\partial p}{\partial x} + \text{div}(\mu \text{grad } \mathbf{U}) + S_M \quad (10)$$

$$\rho \frac{DT}{Dt} = -p \text{div } \mathbf{U} + \text{div}(\Gamma \text{grad } T) + \Phi + S_i \quad (11)$$

Turbulent model:

$$\frac{\partial(\rho k)}{\partial t} + \text{div}(\rho k \mathbf{U}) \quad (12)$$

$$= \text{div} \left[ \left( \frac{\mu_t}{\sigma_k} \text{grad } k \right) \right] + 2\mu_t E_{ij} \cdot E_{ij} - \rho \varepsilon$$

$$\frac{\partial(\rho \varepsilon)}{\partial t} + \text{div}(\rho \varepsilon \mathbf{U})$$

$$= \text{div} \left( \frac{\mu_t}{\sigma_\varepsilon} \text{grad } \varepsilon \right) \quad (13)$$

$$+ C_{1\varepsilon} \frac{\varepsilon}{k} 2\mu_t E_{ij} \cdot E_{ij} - C_{2\varepsilon} \rho \frac{\varepsilon^2}{k}$$

Boundary and initial conditions:

$$q_{wall} = 0,$$

$$u = u_{in}, v = 0, w = 0, \varepsilon = \varepsilon_{in}, k = k_{in}, T = T_{in} \quad (14)$$

$$\varepsilon_{in} = C_\mu^{3/4} \frac{k^{3/2}}{L_e}, k_{in} = \frac{3}{2} (u_{in} I)^2, \quad (15)$$

$$I = \frac{u'}{u} \times 100\%$$

Launder and Spalding [56] proposed the turbulence model constants of  $C_\mu = 0.09$ ,  $C_{\varepsilon 1} = 1.47$ ,  $C_{\varepsilon 2} = 1.92$ ,  $\sigma_k = 1.0$ ,  $\sigma_\varepsilon = 1.3$ .

A turbulent flow model is used to analyze the problem [58] and solved by using ANSYS as a solver in the numerical process. As shown in Figure 3, all walls, ceilings, and floors are adiabatic. The air flowing is the steady-state, the single phase-flow condition with constant properties (Variation of air properties with temperature is excluded), and radiation heat transfer is not considered. The constant inlet temperature and airflow rate are 3.7, 4.2, and 4.7 m<sup>3</sup>/s.

In order to obtain the computation accuracy, the grids independent test is performed with three different grids of 5.0 x 10<sup>5</sup>, 2.0 x 10<sup>6</sup>, and 3.0 x 10<sup>6</sup>. The residual summed is set of 10<sup>-6</sup> for the ended computation. The air temperature of 3.0x10<sup>6</sup>

is finer than that of  $2.0 \times 10^6$  less than 1%, and the grid of  $2.0 \times 10^6$  ensures satisfactory results, as shown in Figure 4.

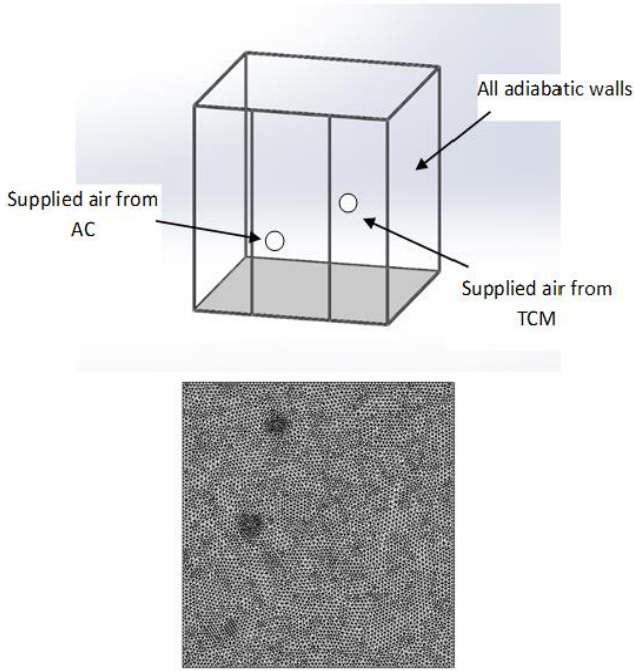


**Figure 3.** Computation domain and grid configuration of the present study

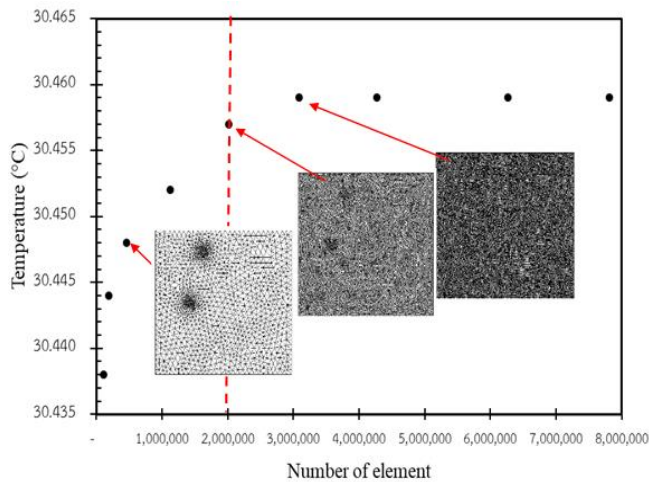


**Figure 4.** Grid independent test

#### 4. RESULTS AND DISCUSSION

The experiment performs for the operating time from 08.00 to 11.00 am, which sets the start air temperature of 30°C. Experiments are done with six different conditions, as shown in Table 2. The inlet airflow rate discharged in the closed room is also an important parameter that affects the cooling effect. Air temperature distributions in the closed room are measured in three levels (each level measured in four positions), as shown in Figure 1(B). Figure 4 illustrates the air temperature variation inside the closed room. Air temperature at 50 cm from the floor is the lowest and increases at a higher distance. Cases IV, V, and VI are the air conditioning system with the thermoelectric cooling module, and cases I, II, and III are without a thermoelectric cooling module. The room temperatures from the air conditioning with the thermoelectric

cooling module (cases IV, V, and VI) are lower than those without the thermoelectric cooling module (cases I, II, and III).

**Table 2.** Operating conditions of the present study

Case Studies	Details
Case I	Air conditioning (AC) turns on without a thermoelectric cooling module (TCM) at an airflow rate of 3.7 m <sup>3</sup> /s
Case II	Air conditioning (AC) turns on without a thermoelectric cooling module (TCM) at an airflow rate of 4.2 m <sup>3</sup> /s
Case III	Air conditioning (AC) turns on without a thermoelectric cooling module (TCM) at an airflow rate of 4.7 m <sup>3</sup> /s
Case IV	Air conditioning (AC) and thermoelectric cooling module (TCM turn on at an airflow rate of 3.7 m <sup>3</sup> /s
Case V	Air conditioning (AC) and thermoelectric cooling module (TCM turn on at an airflow rate of 4.2 m <sup>3</sup> /s
Case VI	Air conditioning (AC) and thermoelectric cooling module (TCM turn on at an airflow rate of 4.7 m <sup>3</sup> /s

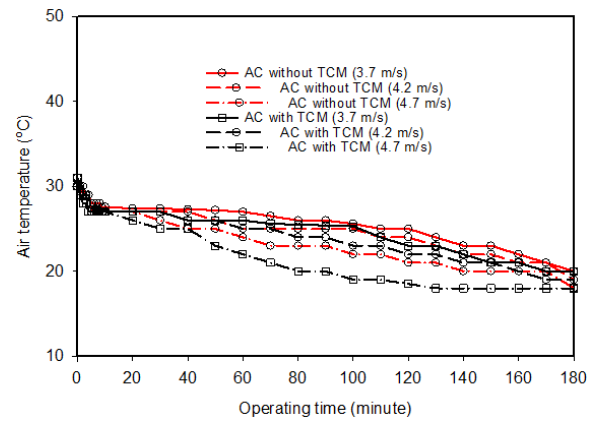


**Figure 5.** Variation of air temperature inside the room

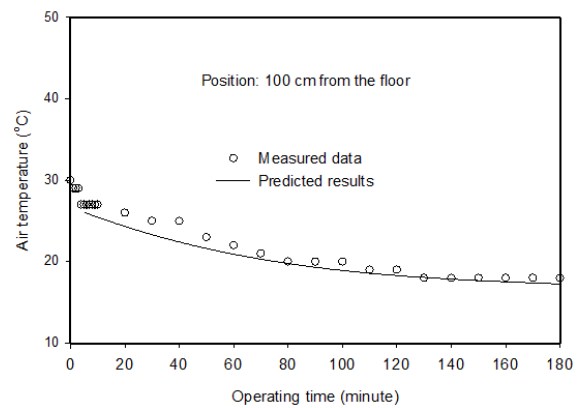


**Figure 6.** Comparison of air temperatures from the predicted results and the measured data of TC with TCM at an airflow rate of 4.7 m<sup>3</sup>/s

It can be seen that the minimum cooling temperature of the system meets about 16-17°C. However, in general, the air conditioning temperature is set as 24°C. If the temperature drops to the set value (24°C), the air conditioning system will stop working. This means that it saves energy. With the thermoelectric cooling module working, the air temperature inside the room drops to the set value faster. The heat removal ability for the air conditioning with the thermoelectric cooling module is removed rapidly at higher axial fan speed. The higher airflow rate gives the air temperature lower than that lower one, as shown in Figure 5. The comparison of the air

temperature obtained from the measured data and the predicted results at the 100 cm positioning from the floor is shown in Figure 6. It is observed that the numerical study is slightly underpredicted and gives errors of 3.77%. This is because of heat transfer from the outside into the room during the experiment. Therefore, the air temperatures in the experiment are higher than the calculated ones. The temperature and velocity distributions of air for the air conditioning (AC) system with the thermoelectric cooling module (TCM) are shown in Figure 7. The horizontal and vertical cross-section planes through the air conditioning system and thermoelectric cooling module are performed and presented. The air temperature inside the room tends to decrease with increasing operating time. The minimum air temperature in the air conditioning system zone is about 16-17°C. The thermoelectric cooling module can reduce air temperature to as low as 18°C. The main supply airflow from the air conditioning system is discharged by centrifugal fans into the room to impinge the opposite wall and then spread into the other air zone inside the room, which this phenomenon is similar to the air flowing from the thermoelectric cooling module. The minimum air temperature occurs at the main airflow of the air conditioning zone and tends to increase in the outer area. The air temperature from the air conditioning is lower than that from the thermoelectric cooling module. The mixing level between the two main airflows (low-temperature zone) and air in the other area depends on two airflow rates through the air conditioning system and the thermoelectric cooling module.

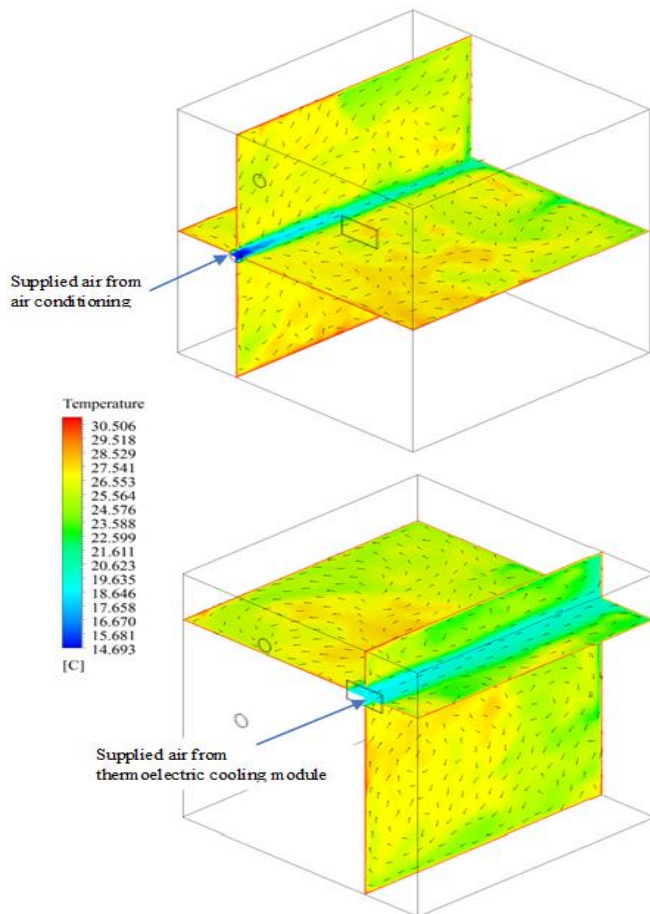


Figure 7. Velocity vector and temperature distribution inside the room for AC with TCM

The axial fan induces the air inside the closed room to flow through the heat sink unit of the thermoelectric cooling module. Therefore, the cooling ability functions the thermoelectric plate and inlet air temperature (inside the closed room). In the beginning, the cooling removal ability of the thermoelectric cooling module is high due to the high-temperature difference. However, the cooling ability decreases because the temperature difference decreases as the operating time continues. Outside air is induced and flows through the air conditioning system. This means that the cooling ability of the air conditioning system depends on outside air temperature, which the cooling ability decreases for the whole operating time range (08.00-11.00 am) as the higher outside air temperature, especially at noon. Therefore, the cooling ability of the air conditioning system with and without the thermoelectric cooling module decrease as the operating time goes on. Reductions in the COP for different operating conditions are shown in Figure 8. The COPs increase with increasing airflow rate, which is the reason mentioned above.

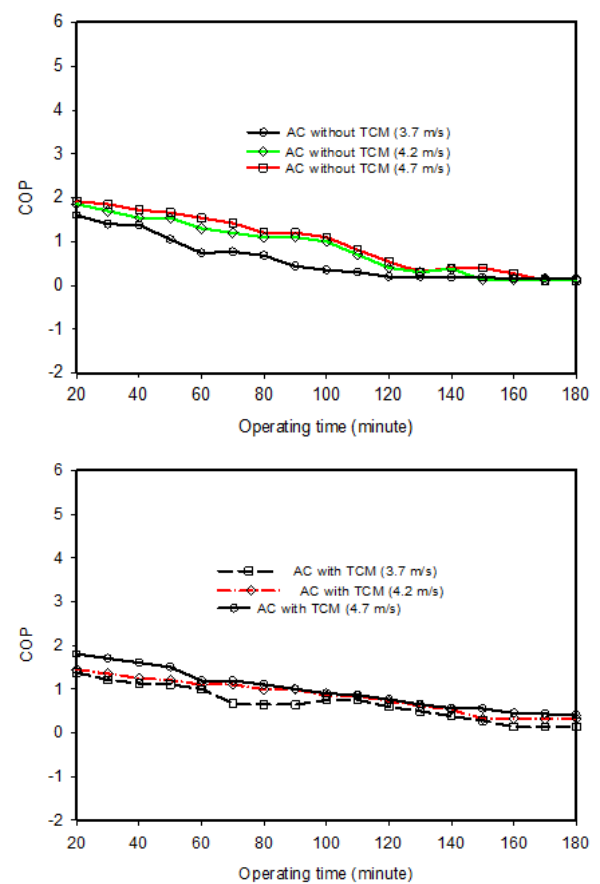


Figure 8. Variation of COP of air conditioning

Figure 9 compares the average COP and EER of the air conditioning system with and without the TCM. It is observed that the average COPs of cases I, II, and III are 1.11, 1.15, and 1.24 for airflow rates of 3.7, 4.2, 4.7 m<sup>3</sup>/s, respectively, whereas the average COPs of cases IV, V, and VI are approximately 1.20 [3.7 m<sup>3</sup>/s], 1.21 [4.2 m<sup>3</sup>/s], and 1.71 [4.7 m<sup>3</sup>/s]. In addition, the EERs of air conditioning systems with thermoelectric cooling modules increase about 7.90%, 5.13%, and 31.84% for airflow rates of 3.7, 4.2, and 4.7 m<sup>3</sup>/s, respectively, as shown in Figure 9.

The COPs obtained from the measured data are compared with those from the predicted results. As shown in Table 3, it

can be found that reasonable agreement is obtained from the comparison and give maximum and minimum errors of 7.63% and 1.75%, respectively. In addition, the predicted results are higher than those from the measured data. This may be due to the heat transfer from the outside into the room during the experiment.

**Table 3.** Comparison of COP from the measured data and the predicted results

Operating modes	COP		%Errors
	Experimental results	Predicted results	
Case I	1.11	1.17	4.82
Case II	1.15	1.21	5.07
Case III	1.24	1.26	1.75
Case IV	1.20	1.25	4.07
Case V	1.21	1.30	6.92
Case VI	1.71	1.85	7.63

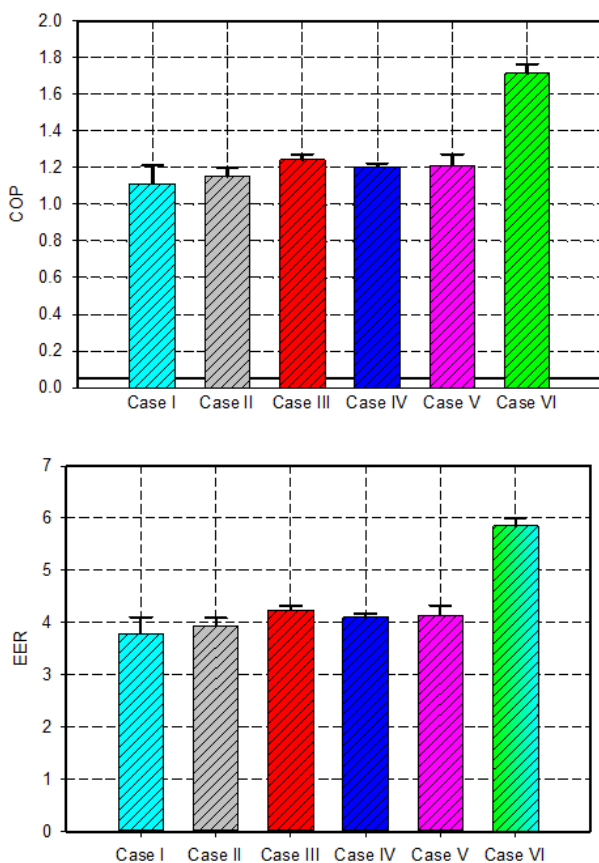


**Figure 9.** Comparison of COP and EER for different operating conditions

## 5. CONCLUSIONS

Air conditioning systems rapidly increase human living standards, resulting in higher energy consumption. However, air conditioning systems have been developed continuously to obtain higher efficiency and lower power consumption. Today, a thermoelectric cooler is applied in many systems. This is because thermoelectric coolers have many advantages, such as having a small scale, easily switching between heating and cooling modes, and a quiet operating environment. The efficiency of the combined small-scale air conditioning and thermoelectric cooling systems driven by solar cells has been

investigated. It is found that the COP and EER of the small-scale air conditioning system have been achieved as compared to without the thermoelectric cooling module. The COPs of air conditioning systems with thermoelectric cooling modules increase about 7.90%, 5.13%, and 31.84% for airflow rates of 3.7, 4.2, and 4.7 m<sup>3</sup>/s, respectively. However, the thermoelectric air-cooling module will need further development in order to get higher thermal efficiency.

## ACKNOWLEDGMENT

The authors thank Srinakharinwirot University for financial support and Udon Thani Rajabhat for place support for this study.

## REFERENCES

- [1] Astrain, D., Vian, J.A., Albizua, J. (2005). Computational model for refrigerators based on Peltier effect application. *Apply Thermal Engineering*, 25: 3149-3162. <https://doi.org/10.1016/j.applthermaleng.2005.04.003>
- [2] Astrain, D., Vian, J.G., Dominguez, M. (2003). Increase of COP in the thermoelectric refrigeration by the optimization of heat dissipation. *Apply Thermal Engineering*, 23: 2183-2200. [https://doi.org/10.1016/S1359-4311\(03\)00202-3](https://doi.org/10.1016/S1359-4311(03)00202-3)
- [3] Hermes, C.J.L., Barbosa J.R. (2012). Thermodynamic comparison of Peltier, Stirling, and vapor compression portable coolers. *Apply Energy*, 91: 51-58. <https://doi.org/10.1016/j.apenergy.2011.08.043>
- [4] Min, G., Rowe, D.M. (2006). Experimental evaluation of prototype thermoelectric domestic-refrigerators. *Apply Energy*, 83: 133-152. <https://doi.org/10.1016/j.apenergy.2005.01.002>
- [5] Dai, Y.J., Wang, R.Z., Ni, L. (2003). Experimental investigation and analysis on a thermoelectric refrigerator driven by solar cells. *Solar Energy Materials and Solar Cells*, 77: 377-391. [https://doi.org/10.1016/S0927-0248\(02\)00357-4](https://doi.org/10.1016/S0927-0248(02)00357-4)
- [6] Dai, Y.J., Wang, R.Z., Ni, L. (2003). Experimental investigation on a thermoelectric refrigerator driven by solar cells. *Renewable Energy*, 28: 949-959. [https://doi.org/10.1016/S0960-1481\(02\)00055-1](https://doi.org/10.1016/S0960-1481(02)00055-1)
- [7] Abdul-Wahab, S.A., Elkamel, A., Al-Damkhi, A.M., Al-Habsi, I.A., Al-Rubai'ey, S.H., Al-Battashi, A.K., Al-Tamimi, A.R., Al-Mamari, K.H., Chutani, M.U. (2009). Design and experimental investigation of portable solar thermoelectric refrigerator. *Renewable Energy*, 34: 30-34. <https://doi.org/10.1016/j.renene.2008.04.026>
- [8] Astrain, D., Martinez, A., Rodriguez, A. (2021). Improvement of a thermoelectric and vapour compression hybrid refrigerator. *Apply Thermal Engineering*, 39: 140-150. <https://doi.org/10.1016/j.applthermaleng.2012.01.054>
- [9] He, Y., Rong, L., Chen, G. (2021). Study on the performance of a solid-state thermoelectric refrigeration system equipped with ionic wind fans for ultra-quiet operation. *International Journal of Refrigeration*, 5: 1-11. <http://doi:10.1016/J.IJREFRIG.2021.06.017>
- [10] Chein, R., Huang, G. (2004). Thermoelectric cooler application in electronic cooling. *Apply Thermal*

- Engineering, 24: 2207-2217. <https://doi.org/10.1016/j.applthermaleng.2004.03.001>
- [11] Zhang, H.Y., Mui, Y.C., Tarin, M. (2010). Analysis of thermoelectric cooler performance for high power electronic packages. *Apply Thermal Engineering*, 30: 561-568. <https://doi.org/10.1016/j.applthermaleng.2009.10.020>
- [12] Naphon, P., Wiriyasart, S. (2009). Liquid cooling in the mini-rectangular fin heat sink with and without thermoelectric for CPU. *Int. Commun. International Communications in Heat and Mass Transfer*, 36: 166-171. <https://doi.org/10.1016/j.icheatmasstransfer.2008.10.002>
- [13] Nnanna, A.G.A., Rutherford, W., Elomar, W., Sankowski, B. (2009). Assessment of thermoelectric module with nanofluid heat exchanger. *Apply Thermal Engineering*, 29: 491-500. <https://doi.org/10.1016/j.applthermaleng.2008.03.007>
- [14] Putra, N., Ferdiansyah, Y., Iskandar, N. (2011). Application of nanofluids to a heat pipe liquid-block and the thermoelectric cooling of electronic equipment. *Experimental Thermal and Fluid Science*, 35: 1274-1281. <https://doi.org/10.1016/j.expthermflusci.2011.04.015>
- [15] Yang, J., Stabler, F.R. (2009). Automotive applications of thermoelectric materials. *Journal of Electronic Materials*, 38: 11892. <https://doi.org/10.1007/s11664-009-0680-z>
- [16] Qinghai, L., Yanjin, W., Pengfei, Z. (2010). A novel thermoelectric air conditioner for a truck cab. *International Conference on Advances in Energy Engineering*. <http://doi.org/10.1109/ICAEE.2010.5557585>
- [17] Chen, C., Mao, L., Lin, T., Tu, T., Zhu, L., Wang, C. (2020). Performance testing and optimization of a thermoelectric elevator car air conditioner. *Case Studies in Thermal Engineering*, 19: 100616. <https://doi.org/10.1016/j.csite.2020.100616>
- [18] Vashisht, S., Rakshit, D. (2021). Recent advances and sustainable solutions in automobile air conditioning systems. *Journal of Cleaner Production*, 329: 129754. <https://doi.org/10.1016/j.jclepro.2021.129754>
- [19] Kim, D., Seo, S., Kim, S., Shin, S., Son, K., Jeon, S., Han, S. (2022). Design and performance analyses of thermoelectric coolers and power generators for automobiles. *Sustainable Energy Technologies and Assessments*, 51: 101955. <https://doi.org/10.1016/j.seta.2022.101955>
- [20] Srivastava, R.S., Kumar, A., Thakur, H., Vaish, R. (2022). Solar assisted thermoelectric cooling/heating system for vehicle cabin during parking: A numerical study. *Renewable Energy*, 181: 384-403. <https://doi.org/10.1016/j.renene.2021.09.063>
- [21] Riffat, S.B., Qiu, G. (2004). Comparative investigation of thermoelectric air conditioners versus vapour compression and absorption air-conditioners. *Apply Thermal Engineering*, 24: 1979-1993. <https://doi.org/10.1016/j.applthermaleng.2004.02.010>
- [22] Cosnier, M., Fraisse, G., Luo, L. (2008). An experimental and numerical study of a thermoelectric air-cooling and air-heating system. *International Journal of Refrigeration*, 31: 1051-1062. <https://doi.org/10.1016/j.ijrefrig.2007.12.009>
- [23] Cheng, T.C., Cheng, C.H., Huang, Z.Z., Liao, G.C. (2011). Development of an energy-saving module via combination of solar cells and thermoelectric coolers for green building applications. *Energy*, 36: 133-140. <https://doi.org/10.1016/j.energy.2010.10.061>
- [24] Gillott, M., Jiang, L., Riffat, S. (2009). An investigation of thermoelectric cooling devices for small-scale space conditioning applications in buildings. *International Journal of Energy Research*, 34: 776-786. <https://doi.org/10.1002/er.1591>
- [25] Arenas A.A., Palacios, R., Rodríguez-pecharromán, R., Pagola, F.L. (2008). Full-size prototype of active thermal windows based on thermoelectricity. *Proceedings of ECT2008e6th European Conference on Thermoelectrics*, Paris, France.
- [26] Vázquez, J., Sanz-Bobi, M.A., Palacios, R., Arenas, A. (2001). An active thermal wall based on thermoelectricity. *Sixth European Workshop on Thermoelectrics*. Freiburg, Germany, Sep 2001.
- [27] Shen, L., Xiao, F., Chen, H., Wang, S. (2013). Investigation of a novel thermoelectric radiant air-conditioning system. *Energy Build*, 59: 123-132. <https://doi.org/10.1016/j.enbuild.2012.12.041>
- [28] Cherkez, R. (2012). Theoretical studies on the efficiency of air conditioner based on permeable thermoelectric converter. *Applied Thermal Engineering*, 38: 7-13. <https://doi.org/10.1016/j.applthermaleng.2012.01.012>
- [29] Miranda, A.G., Chen, T.S., Hong, C.W. (2013). Feasibility study of a green energy powered thermoelectric chip based air conditioner for electric vehicles. *Energy*, 59: 633-641. <https://doi.org/10.1016/j.energy.2013.07.013>
- [30] Shen, L., Tu, Z., Hu, Q., Tao, C., Chen, H. (2017). The optimization design and parametric study of thermoelectric radiant cooling and heating panel. *Applied Thermal Engineering*, 112: 688-697. <https://doi.org/10.1016/j.applthermaleng.2016.10.094>
- [31] Liu, Z., Zhang, L., Gong, G., Luo, Y., Fangfang, M. (2015). Experimental study and performance analysis of a solar thermoelectric air conditioner with hot water supply. *Energy and Buildings*, 86: 619-625. <https://doi.org/10.1016/j.enbuild.2014.10.053>
- [32] Attar, A., Lee, H. (2016). Designing and testing the optimum design of automotive air-to-air thermoelectric air conditioner (TEAC) system. *Energy Conversion and Management*, 112: 328-336. <https://doi.org/10.1016/j.enconman.2016.01.029>
- [33] Li, X., Xie, C., Quan, S., Huang, L., Fang, W. (2018). Energy management strategy of thermoelectric generation for localized air conditioners in commercial vehicles based on 48 V electrical system. *Applied Energy*, 231: 887-900. <https://doi.org/10.1016/j.apenergy.2018.09.162>
- [34] Irshad, K., Habib, K., Algarni, S., BaranSaha, B., Jamil, B. (2019). Sizing and life-cycle assessment of building integrated thermoelectric air cooling and photovoltaic wall system. *Applied Thermal Engineering*, 154: 302-314. <https://doi.org/10.1016/j.applthermaleng.2019.03.027>
- [35] Lou, L., Shou, D., Park, H., Zhao, D., Wu, Y.S., Hui, X., Yang, R., Kan, E.C., Fan, J. (2020). Thermoelectric air conditioning undergarment for personal thermal management and HVAC energy saving. *Energy & Buildings*, 226: 110374. <https://doi.org/10.1016/j.enbuild.2020.110374>

- [36] Tian, X.X., Asaadi, S., Moria, H., Kaood, A., Pourhedayat, S., Jermsittiparsert, K. (2020). Proposing tube-bundle arrangement of tubular thermoelectric module as a novel air cooler. *Energy*, 208: 118428. <https://doi.org/10.1016/j.energy.2020.118428>
- [37] Duan, M., Sun, H., Lin, B., Wu, Y. (2021). Evaluation on the applicability of thermoelectric air cooling systems for buildings with thermoelectric material optimization. *Energy*, 15: 119723. <https://doi.org/10.1016/j.energy.2020.119723>
- [38] Koochi, N., Nasirifar, S., Behzad, M., Cardemil, J.M. (2021). Experimental investigation and performance assessment of a solar-driven thermoelectric unit for localized heating and cooling applications. *Energy & Buildings*, 253: 111517. <https://doi.org/10.1016/j.enbuild.2021.111517>
- [39] Srivastava, R.S., Kumar, A., Sharma, S., Thakur, H., Patel, S., Vaish, R. (2021). Development and applications of thermoelectric based dehumidifiers. *Energy & Buildings*, 252: 111446. <https://doi.org/10.1016/j.enbuild.2021.111446>
- [40] Salehi, R., Jahanbakhshi, A., Golzarian, M.R., Khojastehpour, M. (2021). Evaluation of solar panel cooling systems using anodized heat sink equipped with thermoelectric module through the parameters of temperature, power and efficiency. *Energy Conversion and Management*, 11: 100102. <https://doi.org/10.1016/j.ecmx.2021.100102>
- [41] Han, X., Wang, Y. (2021). Experimental investigation of the thermal performance of a novel split-type liquid-circulation thermoelectric cooling device. *Applied Thermal Engineering*, 194: 117090. <https://doi.org/10.1016/j.applthermaleng.2021.117090>
- [42] Zhou, Y., Yan, Z., Dai, Q., Yu, Y. (2022). Experimental study on the performance of a novel hybrid indirect evaporative cooling/thermoelectric cooling system. *Building and Environment*, 207: 108539. <https://doi.org/10.1016/j.buildenv.2021.108539>
- [43] Saini, A., Watzman, S.J., Bahk, J.H. (2021). Cost-performance trade-off in thermoelectric air conditioning system with graded and constant material properties. *Energy & Buildings*, 240: 110931. <https://doi.org/10.1016/j.enbuild.2021.110931>
- [44] Almodfer, R., Zayed, M.E., Elaziz, M.A., Aboelmaaref, M.M., Mudhsh, M., Elsheikh, A.H. (2022). Modeling of a solar-powered thermoelectric air-conditioning system using a random vector functional link network integrated with jellyfish search algorithm. *Case Studies in Thermal Engineering*, 31: 101797. <https://doi.org/10.1016/j.csite.2022.101797>
- [45] Hommalee, C., Wiriyasart, S., Naphon, P. (2019). Development of cold-hot water dispenser with thermoelectric module systems. *Heat Transfer; Asian Research*, 48(3): 854-863. <https://doi.org/10.1002/htj.21409>
- [46] Wiriyasart, S., Hommalee, C., Prurapark, R., Srichat, A., Naphon, P. (2019). Thermal efficiency enhancement of thermoelectric module system for cold-hot water dispenser; Phase II. *Case Studies in Thermal Engineering*, 15: 100520. <https://doi.org/10.1016/j.csite.2019.100520>
- [47] Wiriyasart, S., Naphon, P., Hommalee, C. (2019). Sensible Air Cool-Warm Fan with Thermoelectric Module Systems Development. *Case Studies in Thermal Engineering*, 13: 100369. <https://doi.org/10.1016/j.csite.2018.100369>
- [48] Naphon, P., Wiriyasart, S. (2019). Experimental and numerical study on the thermoelectric liquid cooler module performance with different heat sink configurations. *Heat and Mass Transfer*, 5: 2445-2454. <https://doi.org/10.1007/s00231-019-02598-x>
- [49] Wiriyasart, S., Hommalee, C., Naphon, P. (2019). Thermal cooling enhancement of dual processors computer with thermoelectric air cooler module. *Case Studies in Thermal Engineering*, 14: 100445. <https://doi.org/10.1016/j.csite.2019.100445>
- [50] Wiriyasart, S., Naphon, P. (2021). Thermal to electrical closed-loop thermoelectric generator with compact heat sink modules. *International Journal of Heat and Mass Transfer*, 164: 120562. <https://doi.org/10.1016/j.ijheatmasstransfer.2020.120562>
- [51] Wiriyasart, S., Suksusron, P., Hommalee, C., Siricharoenpanich, A., Naphon, P. (2021). Heat transfer enhancement of thermoelectric cooling module with nanofluid and ferrofluid as base fluids. *Case Studies in Thermal Engineering*, 24: 100877. <https://doi.org/10.1016/j.csite.2021.100877>
- [52] Sirikasemsuk, S., Wiriyasart, S., Naphon, P. (2021). Thermal cooling characteristics of Li-ion battery pack with thermoelectric ferrofluid cooling module. *International Journal of Energy Research*, 45: 8824-8836. <https://doi.org/10.1002/er.6417>
- [53] Sirikasemsuk, S., Wiriyasart, S., Prurapark, R., Naphon, N., Naphon, P. (2021). Water/Nanofluids Pulsating Flow in Thermoelectric Module for Cooling Electric Vehicle Battery System. *International Journal of Heat and Technology*, 39: 1618-1626. <https://doi.org/10.18280/ijht.390525>
- [54] Vengsungnle, P., Jongpluempiti, J., Srichat, A., Wiriyasart, S., Naphon, P. (2020). Thermal performance of the photovoltaic-ventilated mixed mode greenhouse solar dryer with automatic closed loop control for Ganoderma drying. *Case Studies in Thermal Engineering*, 20: 100659. <https://doi.org/10.1016/j.csite.2020.100659>
- [55] Coleman, H.W., Steele, W.G. (1989). *Experimental and Uncertainty Analysis for Engineers*. John Wiley & Sons, New York.
- [56] Launder, B.E. Spalding, D.B. (1972). *Mathematical Models of Turbulence*. Academic Press.
- [57] Versteeg, H.K., Malalasekera, W. (1995). *An Introduction to Computational Fluid Dynamics: The Finite Volume Method*. Longman, New York.
- [58] Van Doormal, J.P., Raithby, G.D. (1984). Enhancements of the SIMPLEC method for predicting incompressible fluid flows. *Numerical Heat Transfer*, 7: 147-163. <https://doi.org/10.1080/01495728408961817>

## NOMENCLATURE

AC	air conditioning, [-]
COP	coefficient of performance, [-]
$C_p$	specific heat, [kJ/(kg°C)]
I	turbulent intensity, [-]
EER	energy efficiency ratio, [-]
h	enthalpy, [kJ/kg]
$L_e$	equivalent length, [m]
p	pressure, [kPa]



<b>P</b>	power, [kW]
<b>Q</b>	cooling capacity, [kW]
<b>T</b>	temperature, [°C]
<b>TCM</b>	thermoelectric cooling module, [-]
<b>U</b>	velocity vector, [m/s]

#### Greek symbols

$\sigma_\varepsilon$	constants, [-]
$\rho$	density, [kg/m <sup>3</sup> ]
$\sigma_k$	constants, [-]

#### Subscripts

AC	air conditioning
c	cooling
fi	final
fc	fan unit at cold side
fh	fan unit at hot side
in	inlet
st	start
TCM	thermoelectric cooling module
TP	thermoelectric plate